

Supplementary information

for

Photoelectrochemical water splitting by Hematite boosted in heterojunction with B-doped g-C₃N₄ nanosheets and carbon nanotubes

Irfan Khan,^{*a} Tímea Benkó^a, Anita Horváth^a, Shaohua Shen^b, Jinzhan Su^b, Yiqing Wang^b, Zsolt E. Horváth^c, Miklós Németh^a, Zsolt Czigány^c, Dániel Zámbo^c and József Sándor Pap^a

^aHUN-REN Centre for Energy Research, Department of Surface Chemistry and Catalysis, Konkoly-Thege M. Street 29-33, 1121 Budapest, Hungary

^bInternational Research Center for Renewable Energy (IRCREE), State Key Laboratory of Multiphase Flow in Power Engineering (MFPE), Xi'an Jiaotong University, Xi'an, China

^cHUN-REN Centre for Energy Research, Institute of Technical Physics and Materials Science, Konkoly-Thege M. Street 29-33, 1121 Budapest, Hungary

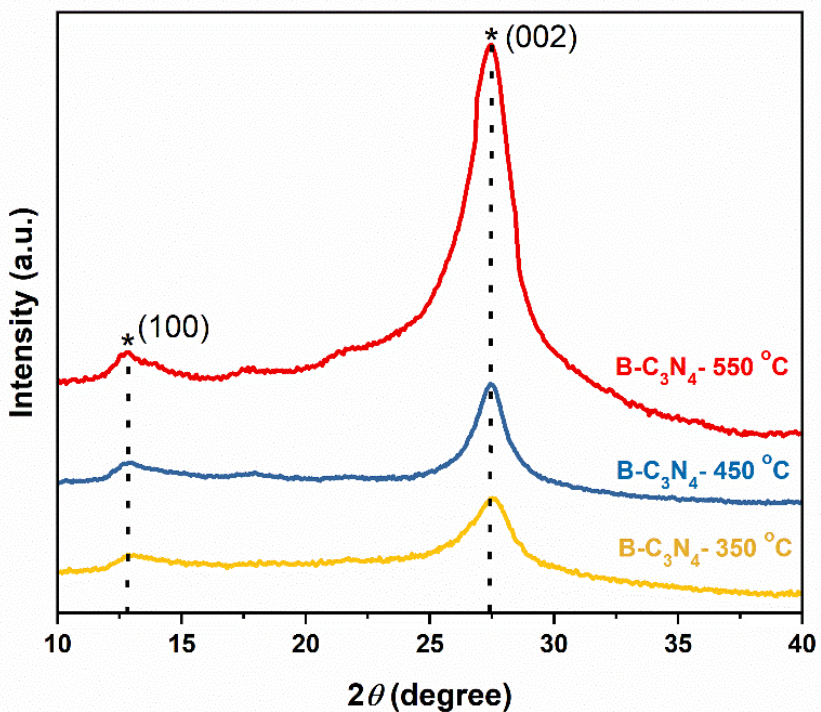


Figure S1. XRD of the B-C₃N₄ samples used in our study with the two expected reflections as discussed in the main text.

Supplementary information

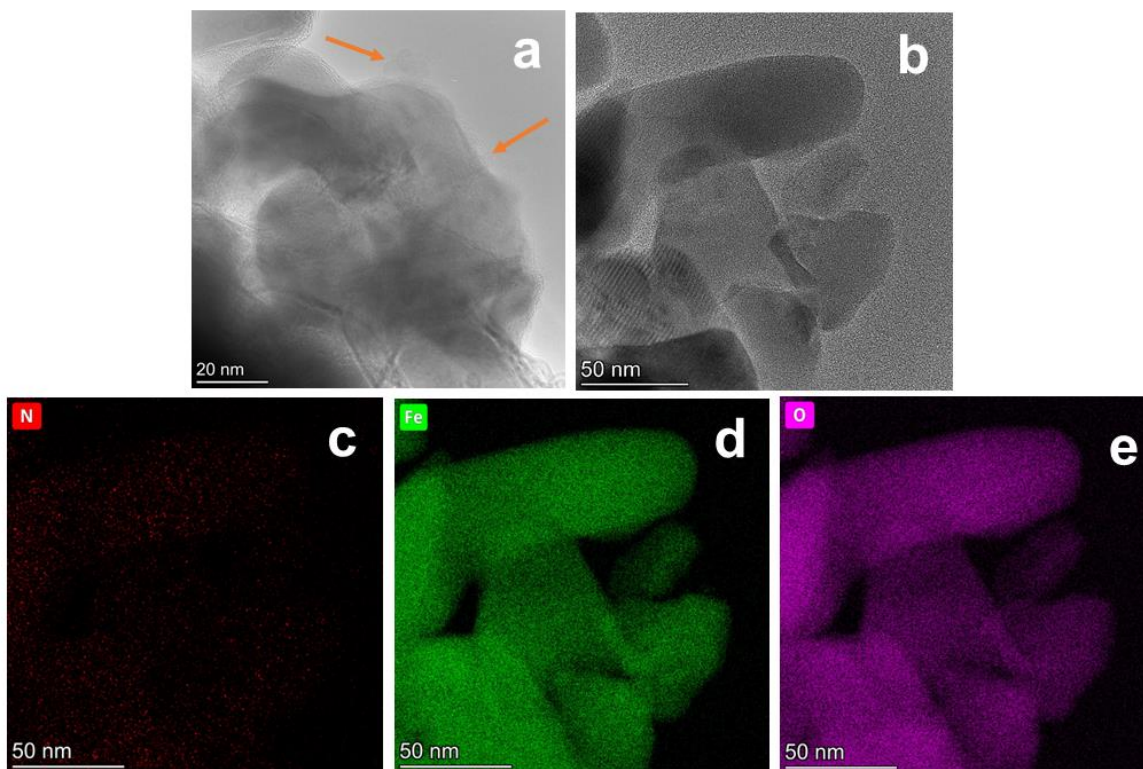


Figure S2. HRTEM and STEM-EDS images of the used α -Fe₂O₃/B-C₃N₄/p-CNT composite (a-b) showed partial crystalline and amorphous structures layered on the α -Fe₂O₃ surface; (c-e) unveiled the homogeneous distribution of nitrogen (N), iron (Fe) and oxygen (O) species across the entirety of the nanorod structures, affirming the successful integration of B-C₃N₄ dopants into the hematite matrix.

Supplementary information

Table S1. Surface atomic concentrations (%) of the used photoanodes were calculated from XPS data.

	Surface atomic concentrations (%)		
	<i>α-Fe₂O₃</i>	<i>α-Fe₂O₃ / B-C₃N₄</i>	<i>α-Fe₂O₃ / B-C₃N₄ / p-CNT</i>
B 1s	1.09	1.03	0.94
C 1s	9.71	10.4	5.7
Cl 2p	0.16	0.2	0.12
Fe 2p	31.94	31.36	35.02
N 1s	0.36	1.09	0.73
Na 1s	2.37	1.89	1.74
O 1s	52.43	52.17	54.42
S 2p	0.91	1.26	1.1
Ti 2p	1.03	0.61	0.23

Supplementary information

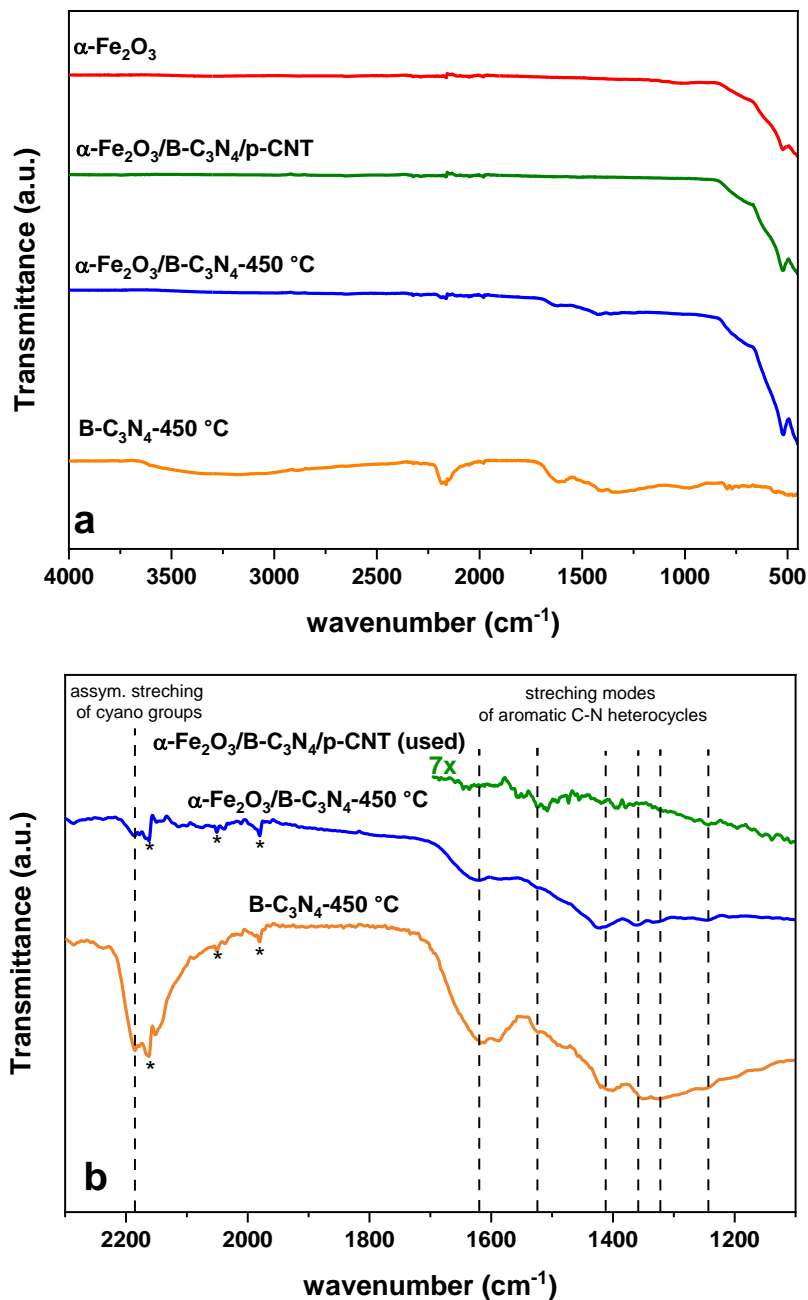


Figure S3. (a) ATR-IR spectra of as-synthesized $\text{B-C}_3\text{N}_4\text{-}450\text{ }^\circ\text{C}$, $\alpha\text{-Fe}_2\text{O}_3$ and $\alpha\text{-Fe}_2\text{O}_3/\text{B-C}_3\text{N}_4\text{-}450\text{ }^\circ\text{C}$ (enriched twice in $\text{B-C}_3\text{N}_4\text{-}450\text{ }^\circ\text{C}$ for the analysis), and the used $\alpha\text{-Fe}_2\text{O}_3/\text{B-C}_3\text{N}_4\text{-}450\text{ }^\circ\text{C}/\text{p-CNT}$ photoanodes; (b) corresponding magnified range of 1100–2300 cm^{-1} . Characteristic stretching modes correspond with a more detailed analysis of $\text{B-C}_3\text{N}_4$, in the ESI of ref. [47]. Asterisks assign artefacts of the diamond detector of the ATR.

Supplementary information

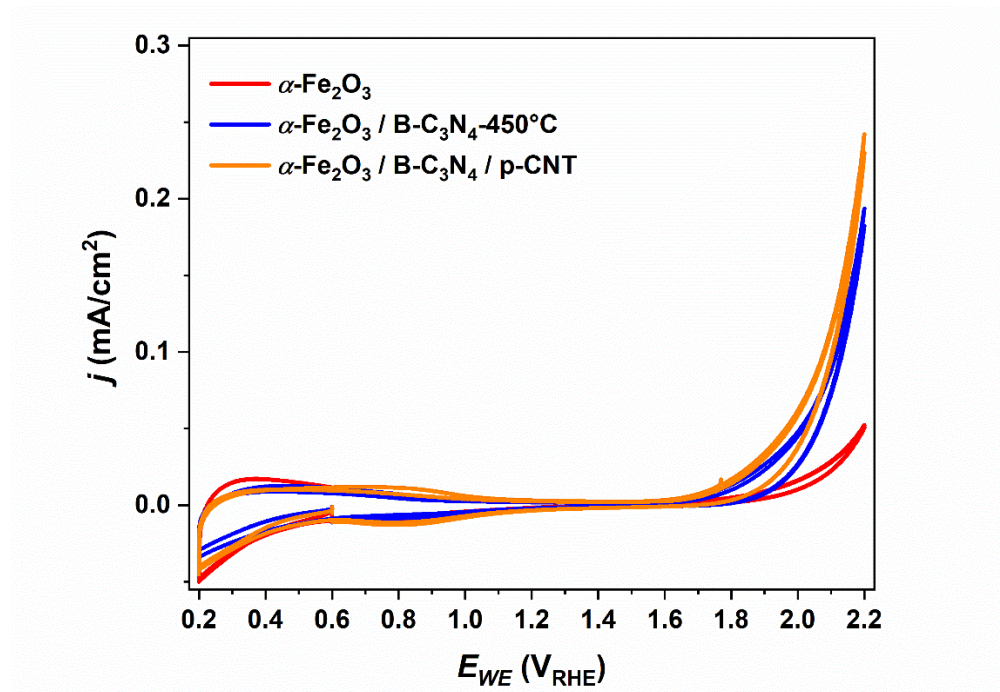


Figure S4. Cyclic voltammetry of the photoanodes used in photoelectrochemistry as shown in Figure 4, recorded in the dark, 2 cycles at 5 mVs⁻¹ in 0.1 M Na₂SO₄ at pH 7.

Supplementary information

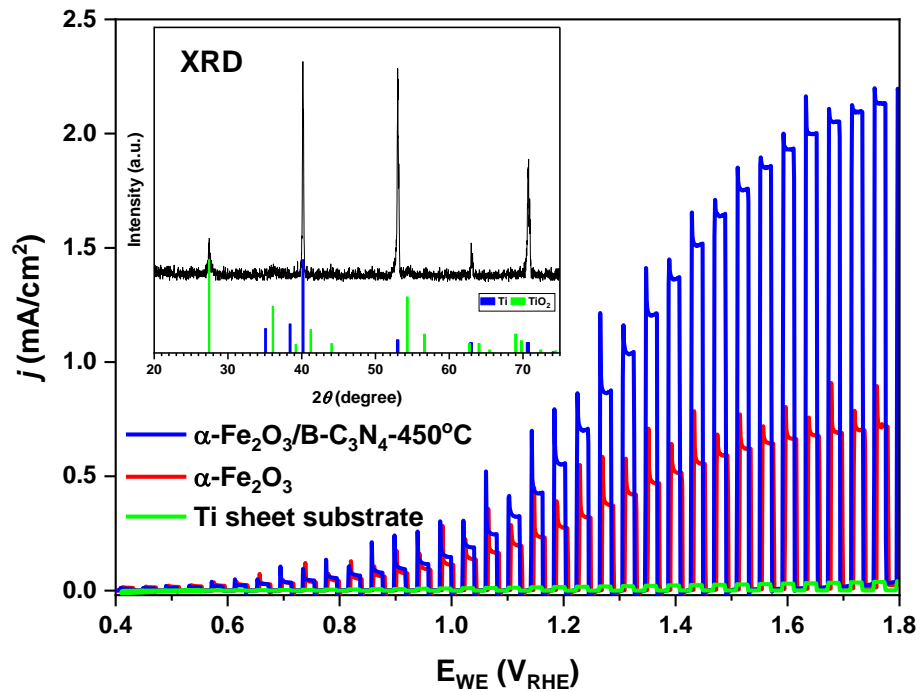


Figure S5. Comparative Linear sweep voltammetry plots between uncoated Ti sheet, pristine α -Fe₂O₃, α -Fe₂O₃/B-C₃N₄-450 °C obtained in 0.1 M Na₂SO₄ at pH 7. The inset shows the XRD patterns of the uncoated Ti substrate.

Supplementary information

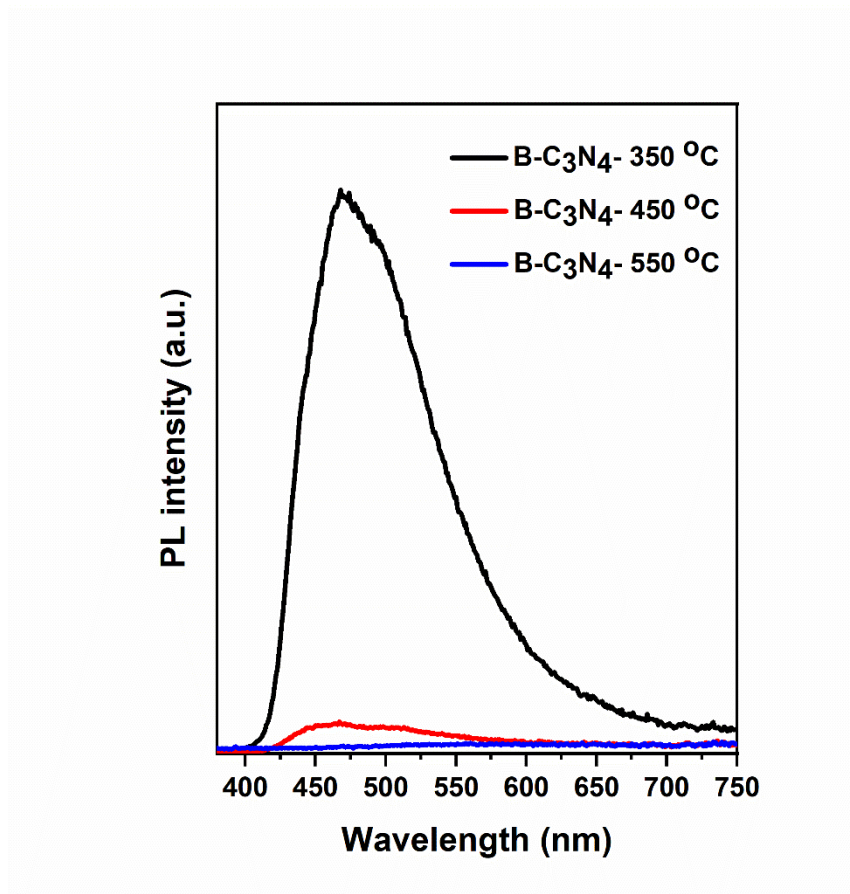


Figure S6. PL spectra of B-C₃N₄ samples at different heat-treatment temperatures.

Supplementary information

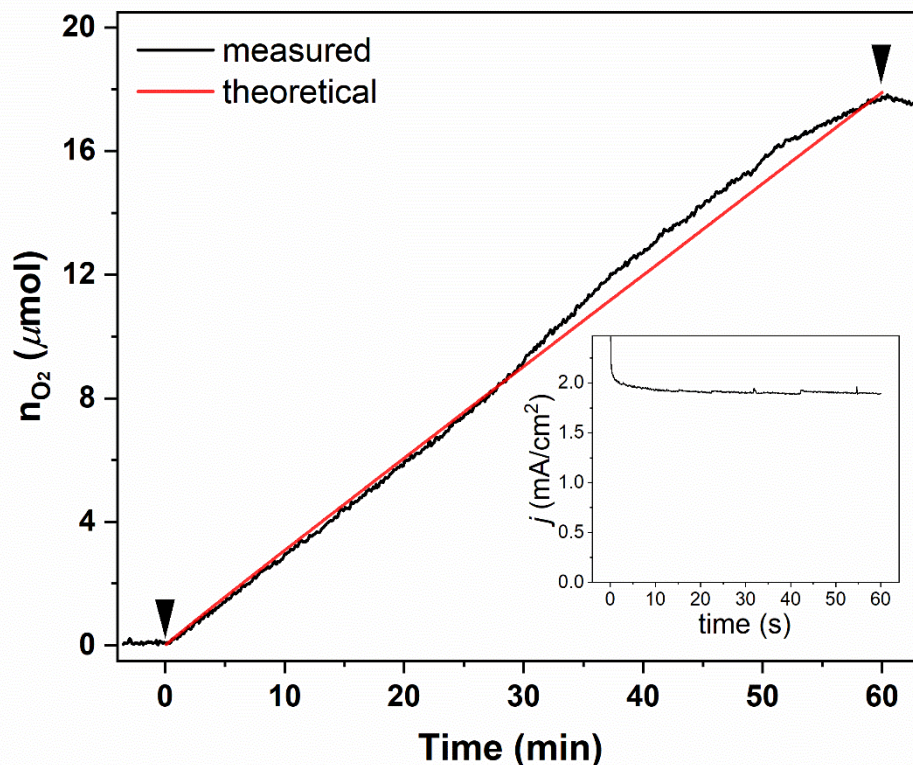


Figure S7. Detected oxygen (black line) and the theoretical amount (red line) in the course of a 1-hour CPE experiment at 1.7 V_{RHE} reference electrode and irradiation at 100 mW cm^{-2} in 0.1 M Na_2SO_4 at pH 7 using the $\alpha\text{-Fe}_2\text{O}_3/\text{B-C}_3\text{N}_4\text{-450 } ^\circ\text{C}/\text{p-CNT}$ photoanode. The theoretical amount of produced oxygen was calculated from the charge as $n_{O_2} = Q/4F$, where n is the molar amount of O_2 , Q is the passed charge in Coulombs, F is the Faraday constant, 96485 C/mol. The black marks indicate the start and the end of the CPE experiment. **Inset:** current density during the experiment.

Supplementary information

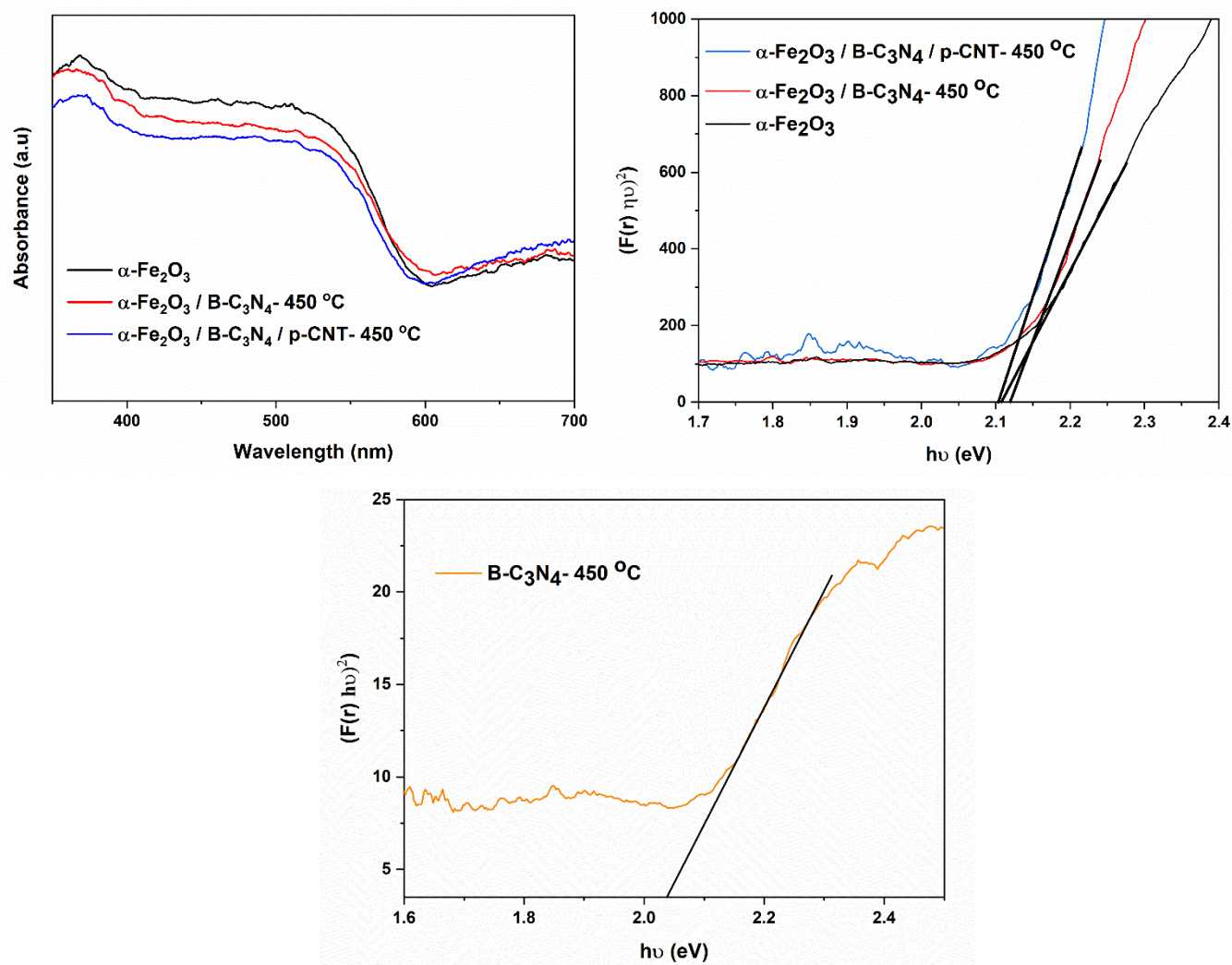


Figure S8. Optical absorbance spectra (DRS) and Tauc plots for the samples as indicated in the legend. The optical absorption ability of $\alpha\text{-Fe}_2\text{O}_3/\text{B-C}_3\text{N}_4\text{-450 }^\circ\text{C}/\text{p-CNT}$ was unchanged, and the remarkable PEC enhancement should be attributed to the surface charge property modification by $\text{B-C}_3\text{N}_4\text{-450 }^\circ\text{C}$ and p-CNT decoration. The UV-vis spectra have very little difference among all the photoanodes, indicating the negligible influence of $\text{B-C}_3\text{N}_4\text{-450 }^\circ\text{C}$ and/or p-CNT decoration on the optical absorption of hematite due to the low loadings. The absorption edges of $\alpha\text{-Fe}_2\text{O}_3$, $\alpha\text{-Fe}_2\text{O}_3/\text{B-C}_3\text{N}_4\text{-450 }^\circ\text{C}$, and $\alpha\text{-Fe}_2\text{O}_3/\text{B-C}_3\text{N}_4\text{-450 }^\circ\text{C}/\text{p-CNT}$ are located *ca.* 590 nm, and the corresponding bandgaps (E_g) of the corresponding samples are calculated by Tauc method to be *ca.* 2.10 eV and 2.04 eV for $\text{B-C}_3\text{N}_4\text{-450 }^\circ\text{C}$.

Supplementary information

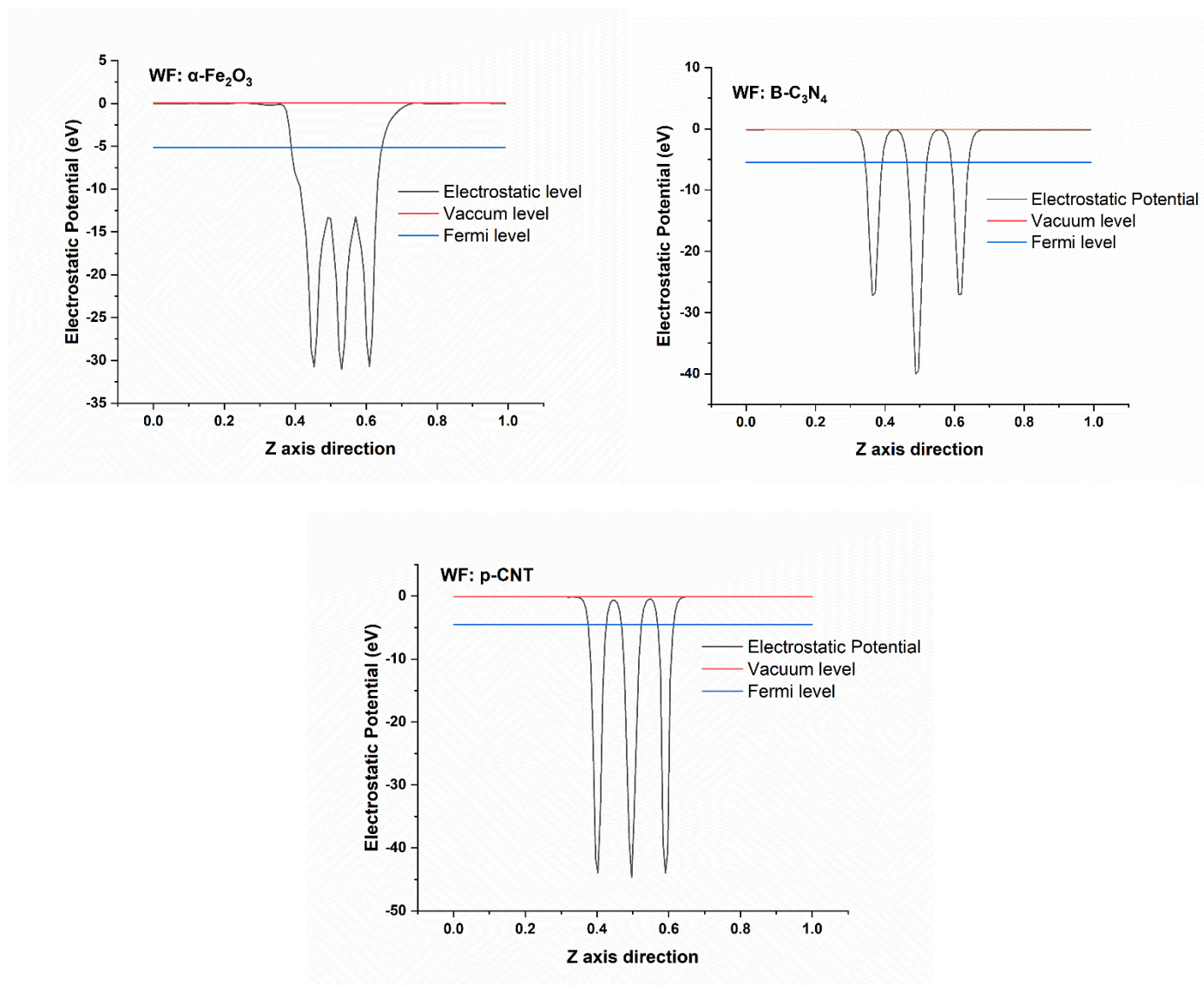


Figure S9. The work functions as calculated for α -Fe₂O₃, B-C₃N₄, and p-CNT are 5.18, 5.39, and 4.18 eV.